

We are IntechOpen, the world's leading publisher of Open Access books Built by scientists, for scientists

6,900

Open access books available

186,000

International authors and editors

200M

Downloads

Our authors are among the

154

Countries delivered to

TOP 1%

most cited scientists

12.2%

Contributors from top 500 universities



WEB OF SCIENCE™

Selection of our books indexed in the Book Citation Index
in Web of Science™ Core Collection (BKCI)

Interested in publishing with us?
Contact book.department@intechopen.com

Numbers displayed above are based on latest data collected.
For more information visit www.intechopen.com



Novel Microbial System Developed from Low-Level Radioactive Waste Treatment Plant for Environmental Sustenance

Shaon Ray Chaudhuri, Jaweria Sharmin,
Srimoyee Banerjee, U Jayakrishnan, Amrita Saha,
Madhusmita Mishra, Madhurima Ghosh,
Indranil Mukherjee, Arpita Banerjee,
Kamlesh Jangid, Mathummal Sudarshan,
Anindita Chakraborty, Sourav Ghosh, Rajib Nath,
Maitreyi Banerjee, Shiv Shankar Singh,
Ajoy Krishna Saha and Ashoke Ranjan Thakur

Additional information is available at the end of the chapter

<http://dx.doi.org/10.5772/63323>

Abstract

A packed bed bioreactor efficiently treated low-level radioactive waste for years with a retention time of 24 h using acetate as the sole carbon source. However, there was generation of dead biomass. This bioreactor biomass was used to develop a bacterial consortium, which could perform the function within 4 h while simultaneously accumulating nitrate and phosphate. The dead mass was negligible. Serial dilution technique was used to isolate the world's first pure culture of a nitrate accumulating strain from this consortium. This isolate could simultaneously accumulate nitrate and phosphate from solution. Its ability to form biofilm helped develop a packed bed bioreactor system for waste water treatment, which could optimally remove 94.46% nitrate within 11 h in batch mode while 8 h in continuous mode from waste water starting from 275 ppm of nitrate. The conventional approach revealed the strain to be a member of genus *Bacillus* but showed distinct differences with the type strains. Further insilico analysis of the draft genome and the putative protein sequences using the bioinformatics tools revealed the strain to be a novel variant of genus *Bacillus*. The sequestered nitrate and phosphate within the cell were visualized through electron microscopy and explained the reason behind the ability of the isolate to accumulate 1.12

mg of phosphate and 1.3 gm of nitrate per gram of wet weight. Transcriptome analysis proposed the mechanism behind the accumulation of nitrate and phosphate in case of this novel bacterial isolate (MCC 0008). The strain with the sequestered nutrients work as biofertilizer for yield enhancement in case of mung bean while maintaining soil fertility post-cultivation.

Keywords: nitrate accumulation, packed bed biofilm reactor, *Bacillus* sp MCC 0008, insilico analysis, transcriptome analysis, radioactive effluent

1. Introduction

All ore mining produce waste rock that in turn may produce acid mine drainage (AMD), due to the presence of sulfides. The waste generated is treated by physico-chemical means and is either stored in engineered containments or in open surface based on the nature of the effluent. Only limited information is available about effects of microbial processes used for similar purposes during large-scale operation. In addition, the mining itself and processing are often associated with a wide range of potential human health risks. Surface and underground mining generate a large volume of waste rock, which may contain only very little uranium but has fission products, for example, radium (radioactive) or lead (highly toxic) that is left behind as a waste. The second step is a process, known as the milling of the ore in which the rocks are crushed and ground. Chemical leaching follows and over 50% of uranium ore is obtained with classic mining methods. Water used in this process that cannot be recycled within a processing plant as well as excess water from a mine needs to be removed or treated to meet environmental requirements. The multistep process of recovery includes neutralization of the effluents, precipitating any metals, and reducing the uranium and radium content. [1–3]. This treatment depends upon the uranium recovery process, chemicals used, and contaminant ores. Water recovered may get recharged as groundwater or is either discharged or used for plant operations. Often this water needs further treatment before it could be reused or discharged for removal of contaminants. The multistep process begin with coagulating or precipitating heavy metals followed by neutralizing acids, or adjusting pH and then precipitating radium with barium chloride. The water treatment process is often followed by additional “clarification” or “polishing” steps using clarifiers, sand filters, and even reverse osmosis. The alternative option might be to use microbial bioremediation using sulfate-reducing bacteria [4].

The foremost source of waste generation occurs during nuclear fuel cycle operations that comprises of facilities to purify, convert, and enrich uranium from mining and milling and to manufacture fuel elements for nuclear reactor and gives rise to a variety of materials and product outputs [2, 3]. Enrichment of radioactive ore involves use of chemicals which lead to high levels of nitrate in the effluent.

The effluent generated cannot be discharged into the environment without treatment. The physicochemical treatment is expensive and economically not feasible during large-scale operation. Hence, biological options were sought. The problem in hand was to develop a microbial process, which could efficiently treat low-level radioactive waste containing nitrate

generated from ore enrichment. Nitrate being a common pollutant in municipal as well as agricultural waste water, municipal sewage was passed through corrugated sheets of a packed bed reactor to develop a biofilm-based bioreactor that could treat low-level radioactive effluent within 24 h on a continuous basis [5] using acetate as the sole carbon source. However, dead mass was generated during the operation. The biomass was characterized [5] and further enrichment in nitrate broth (HiMedia M439) resulted in isolation of the fastest nitrate removing consortium. This consortium was further characterized to yield the world's first nitrate accumulating pure culture [11] of a *Bacillus* sp. with immense application in terms of waste water treatment, plant growth promotion with seed quality enhancing ability. A combined approach of insilico and conventional analysis revealed the strain to be a novel species of genus *Bacillus*. In this chapter, we present the characterization of this novel isolate involved in bioremediation of soluble nitrate.

2. Consortium development and characterization

Nitrate removal from the medium by the bacteria was the primary step for selecting a consortium for nitrate removal. Either an assimilatory or a dissimilatory pathway results in nitrate removal from solution [6]. An alternative pathway for the nitrate removal was through nitrate accumulation, as evident in isolates from genus *Beggiatoa*, *Thiomargarita*, and *Thioploca*. Mussmann et al. [7] proposed a vacuolar nitrate accumulation mechanism linked to proton translocation in *Beggiatoa* sp. from marine origin. The bioreactor biomass treating low-level radioactive waste was selected as inoculum because it solely treated nitrate as a pollutant and would thus have stronger nitrate reducers/accumulators due to the constant exposure to nitrates in radioactive waste water. The consortium (BN7) developed in nitrate broth under aerobic condition reduced the nitrate within the range of 25–37°C temperature and pH 6–11. The consortium could form a biofilm with an optical density of 0.34. Conventionally, an optical density from 0.2 to 0.35 at 620 nm indicates a structured biofilm formation [8]. The biofilm formation was found to be strengthened (0.64) upon application of phytochemicals from



Figure 1. Picture of the biofilm-based packed bed bioreactor developed using the aerobic consortium BN7.

Mentha spicata. These results were validated by calculating the t value (25.23) for 19 df with a 95% confidence level using a two-sample one-tailed t -test with equal variance to yield a p value of 2.24025 E-16. The consortium was used to develop a packed bed biofilm bioreactor (Figure 1) for nitrate and phosphate removal in a continuous system.

The inoculum standardization indicated 10% of the parent culture as optimum for biofilm development. This consortium reduced 97.44% nitrate from the medium within 4 h (Figure 2) while simultaneously reducing 48.2% phosphate during incubation in a biofilm-based bioreactor. This consortium could reduce 500 ppm and 1000 ppm nitrate load within 7 and 5 h, respectively. Nitrate concentrations between 1500 and 4000 ppm could be reduced by 99% within 4 h (Figure 2), and 5000 ppm nitrate was reduced by 80.5% after treating for 11–12 h and 99.62% after 24 h. The correlation coefficient was -0.53173 , which signifies no direct correlation between the initial nitrate load and bioreactor reduction for the range tested in this study. The above data show the aerobic consortium (BN7) to perform the fastest nitrate removal by a microbial system to the best of our knowledge.

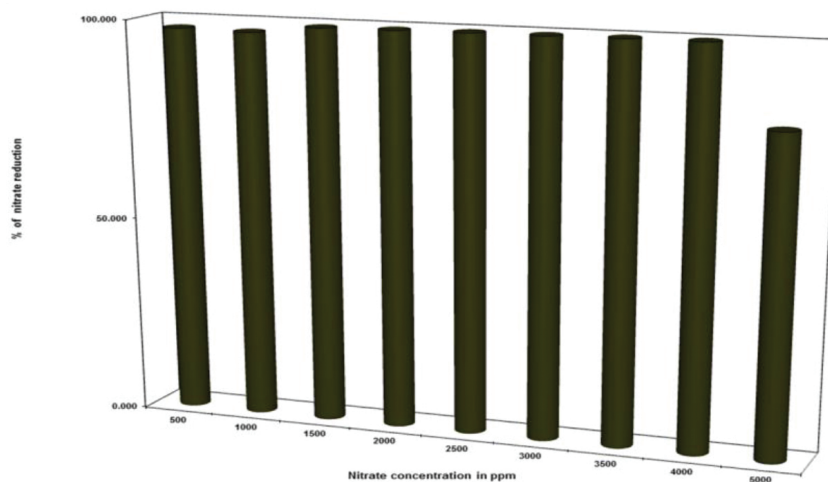


Figure 2. Graph representing the ability of the aerobic consortium BN7 in the packed bed bioreactor (depicted in Figure 3) to reduce nitrate from the medium within 4 h of incubation at room temperature with different initial nitrate load.

On further analysis, this consortium was found to accumulate both nitrate and phosphate simultaneously (2.84 gm/gm wet weight for nitrate and 1.14 mg/gm wet weight for phosphate). Cd, Sr, and Ce inhibited the bacterial growth even at a concentration of 0.1 mM, whereas Co and Zn were inhibitory at 0.5 mM. For Cu, Fe, and Zn salts, lower concentrations had minimal impact on the nitrate reduction, and the reduction efficiency in the presence of Pb salts was at par with the control set. After 4 h of growth, 0.5 mM of Pb salts decreased the reduction efficiency by only 3%. Moreover, the nitrate reduction in the presence of Cu salts after 2 h was higher than for the control (37% in Cu-treated cells compared to 8.5% in control), which can be attributed to the presence of *nirK*, a Cu-dependent nitrate reductase gene. The two-sample one-tailed paired t -test for means was 21.73 for 2 df and at 95% confidence level; the corresponding p value was 0.001. Therefore, the nitrate reduction enhancement in the presence of

Cu was significant. However, the extent of this reduction decreased with increasing time due to the toxic effect of the metal on the microbes. For metals such as Fe, 0.1 mM and 0.5 mM inhibited the reduction by 4–6%, and similarly, 0.1 mM of Zn reduced the efficiency by 3–5%. The negative impact of metals on the reduction efficiency was significant for Co and Cr salts. For the Co treatment, the reduction after 4 h of growth dropped by 50% and 73% relative to the untreated cells for concentrations of 0.1 and 0.5 mM, respectively. Under similar growth conditions, decreasing the Cr salt concentration decreased the nitrate reduction by 30% while increasing the concentration decreased the reduction efficiency by 46% relative to the control cells. The Energy Dispersive X ray Fluorescence (EDXRF) analysis confirmed the metal accumulation in the biomass with the highest accumulation being for Pb (1200 ppb) followed by Cu (180 ppb), Cr (100 ppb), and Co (15 ppb). A single-factor ANOVA yielded a *p* value of 1.58 E–05 with an *F* of 13.90 and critical *F* of 2.70 for 22 df at a 95% confidence level. Hence, the difference in accumulation upon varied metal treatment was significant for BN7. A consortium capable of growing and accumulating such metals can be used for the bioremediation of nitrate and metal co-contaminants.

Preservation experiment revealed both subculture maintenance and glycerol stock storage at –80°C (two months storage) to be equally efficient with nitrate reduction efficiency of 94% and 92%, respectively, after 12 h of growth for BN7. Preserving the culture as a streak plate or stab reduced the efficiency to approximately 88%. The lyophilized form was less efficient relative to the other three storage methods. Thus, using a glycerol stock could be an efficient strategy for the long-term maintenance of the microbial consortium. At the molecular level, the BN7 harbored members which closely resembled *Pseudomonas* sp. (20%), *Azoarcus* sp. (31%), uncultured bacterium (46%) and *Bacillus* sp. (3%). The GenBank accession numbers were GU644465 to GU644489. A phylogenetic analysis was performed using the neighbor joining method (**Figure 3**) as stated above. The low Shannon diversity index value (0.39) confirms selective enrichment using a specific medium for nitrate reducers. An equitability index value (0.83) near 1 indicates that the different varieties observed were evenly distributed throughout the community. The genus *Pseudomonas* and *Bacillus* could be involved in the phosphate accumulation and nitrate reduction. Hence, a microbial consortium was developed which was acclimatized to low-level radioactive waste and could remove nitrate from it within 4 h of incubation at room temperature while generating little dead mass.

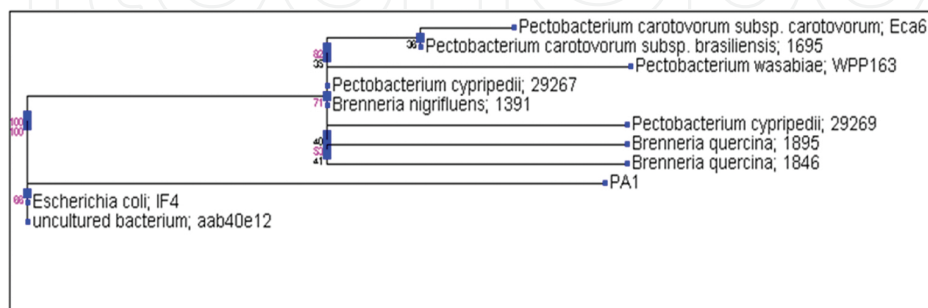


Figure 3. Phylogenetic tree depicting the position of one of the clones from BN7 constructed using the neighbor joining method.

3. Purification of nitrate accumulator and its characterization

Nitrate removal by denitrification and assimilation is well documented for bacterial species. Nitrate accumulation by bacterial genus *Beggiatoa*, *Thioploca*, and *Thiomargarita* [9, 10] is relatively a rare phenomenon. Moreover, all reports of such accumulation are in a mixed form or from environmental mixed samples [9, 10]. Before this study, no pure culture of a nitrate accumulator was reported. Serial dilution and streaking on nitrate agar plates were used to isolate the only pure culture of *Bacillus* sp. MCC0008 [11]. Among the pure strains isolated, MCC0008 was found to be a Gram-positive *Bacillus* (**Figure 4a**). Fatty Acid Methyl Ester (FAME) (0.733) as well as Phospholipid-Derived Fatty Acid (PLFA) analysis revealed similarity with *Bacillus cereus*. MCC0008 shows terminal endospore formation like *Bacillus subtilis* and unlike *Bacillus cereus* (which shows central endospore). Paraspore is absent, while the size is 1.85 μm by 0.899 μm . It has a generation time of 21.4 min and shows terminal endospore location. **Table 1** shows the characteristics of the isolate.

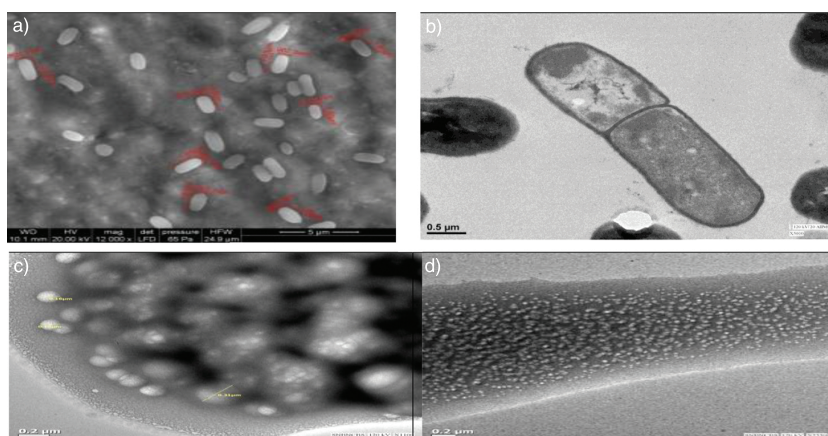


Figure 4a. (a) ESEM micrograph taken using ESEM, FEI QUANTA 200 MARK 2. (b) TEM micrograph taken using TEM, 120 kV, 5000 \times magnification. (c) Phosphate granules of 0.13–0.59 μm in the periphery of cells when grown in low phosphate concentration. (d) Phosphate accumulation throughout the cell when grown at high phosphate concentration.

Enzyme production	Catalase, oxidase, protease, amylase, lipase, DNase positive, lecithinase negative
Carbohydrate utilization	It utilizes dextrose, trehalose, esculin, glycerol, maltose
Plant growth promotion traits	Phosphatase and ammonia production positive, indole acetic acid, hydroxymate siderophore and hydrogen cyanide production negative
Antibiotic sensitivity	Sensitive to ciprofloxacin, norfloxacin, cephadroxil, neomycin, gentamycin, doxycycline hydrochloride Resistant to metronidazole, rifampicin, ampicilin, trimethoprim, roxythromycin, cloxacilin, ceftazidime

Table 1. Characteristics of *Bacillus* sp. MCC0008.

The transmission electron micrographs clearly revealed the presence of vacuoles (**Figure 4b**) which has earlier been reported for nitrate accumulators. This indicates the possibility that the isolate is a nitrate accumulator. The nitrate accumulation study following sonication-based lysis of the harvested pellet and measurement of released nitrate from the intracellular cell free supernatant as per the method of Cataldo et al. [12] exhibited nitrate accumulation of up to 1278.66–1302.122 ppm/gm (0.021 M) of wet weight. It is less than the extent of accumulation reported for *Beggiatoa* but is the first pure isolate of a nitrate accumulator and also the first *Bacillus* reported to perform such function. The isolate accumulated 1115.25 µg/gm of wet weight of phosphate. The extent of phosphate accumulation was higher than that reported by type strain of *Acinetobacter baumannii*. The reason behind this enhanced efficiency was revealed by Transmission electron microscopy of whole cells which showed through and through accumulation of polyphosphate granules in this strain when grown in nitrate broth overnight with high phosphate concentration (**Figure 4c and d**).

The strain showed polysaccharide formation starting from the fourth hour that continued till the eighth hour. This property might provide the benefit of attachment to suitable surfaces to the strain. Active log-phase culture was used to determine whether the isolate could form biofilm according to the method of Martin et al. [8].

Different percentages (1%, 2%, 4%, 6%, 8%, 10%, 15%) of actively growing culture were inoculated in nitrate broth into small falcon containing identical number of plastic rachig rings. The performance in terms of nitrate and phosphate removal was checked for repeated recharges with sterile nitrate broth. The isolate showed good biofilm formation with 10% inoculum being the optimum. The biofilm formation showed saturation by eleventh hour. Optimum performance in terms of nitrate reduction was also observed in the eleventh hour (**Figure 5**). This optimization was further utilized for immobilization of the isolate in the reactor.

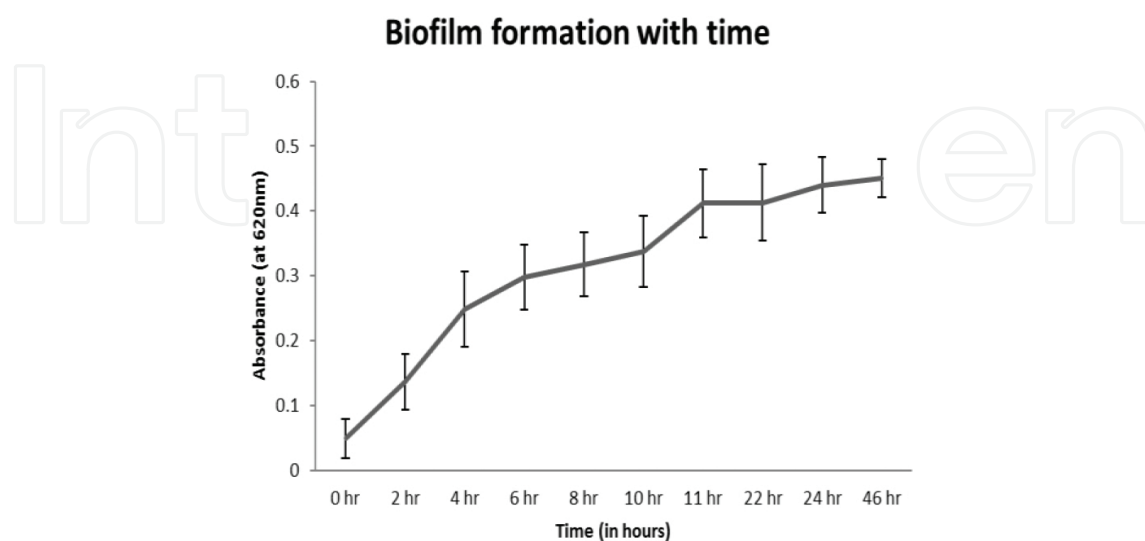


Figure 5. Extent of biofilm formation with time. The saturation was observed after 11 h of incubation.

Accompanied by this, the isolate's ability for active biofilm formation was checked by assaying the supernatant in the tissue culture plate for nitrate and phosphate removal. By this, the time needed for biofilm formation along with optimal functioning in terms of nitrate and phosphate removal was determined to be 11 h for nitrate and 22 h for phosphate (Figure 6).

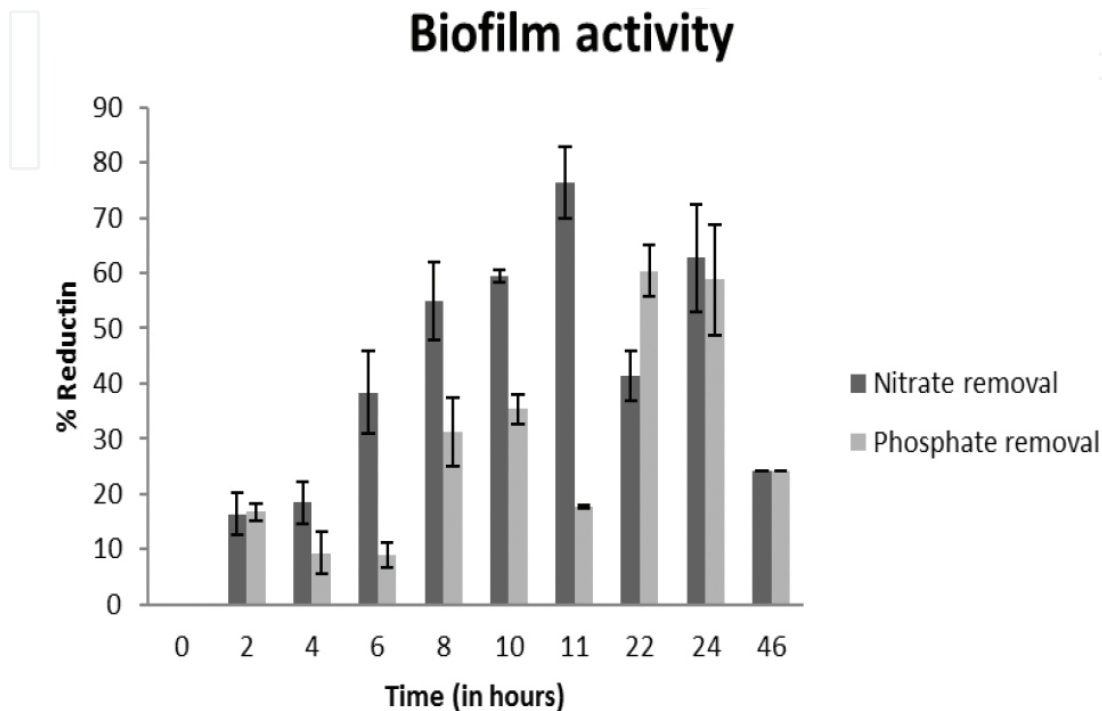


Figure 6. Optimization of time of incubation for biofilm performance.

Since the isolate grows as biofilm, it could be used for setting up of a biofilm-based bioreactor for continuous waste water treatment in terms of nitrate removal. However, a prerequisite for it was to design the minimal growth condition for the same. This would ensure that enrichment culture components would not be needed to run the process and in turn the influent would not add to the COD load of the effluent. Dextrose, glycerol, and citric acid were chosen to check the growth of MCC0008 in minimal condition. The isolate showed the best growth in glycerol, and hence, it was further utilized as the carbon source to determine the optimum percentage of carbon source for growth as well as performance. One percentage of glycerol showed the optimum growth as well as nitrate and phosphate removal under minimal condition. Hence, 1% of glycerol was standardized as the carbon source for the isolate for further studies in packed bed bioreactor.

The comparison of the isolate's activity under different oxygen availability in the eighth hour after inoculation revealed that the isolate performed optimally in aerobic condition followed by anaerobic condition. Oxygen depletion in anaerobic state resulted in a decrease in activity. Highest amount of nitrate reduction and subsequent conversion to ammonia was also in aerobic state due to the assimilatory pathway. Substantial accumulation also occurred in

aerobic state so that the accumulated nitrate could be used as terminal electron acceptor in oxygen-depleted state.

In the 5 L suspended bioreactor, the strain grew exponentially up to 5 h with 65% denitrification and phosphate removal taking place within the fourth hour (Figure 7).

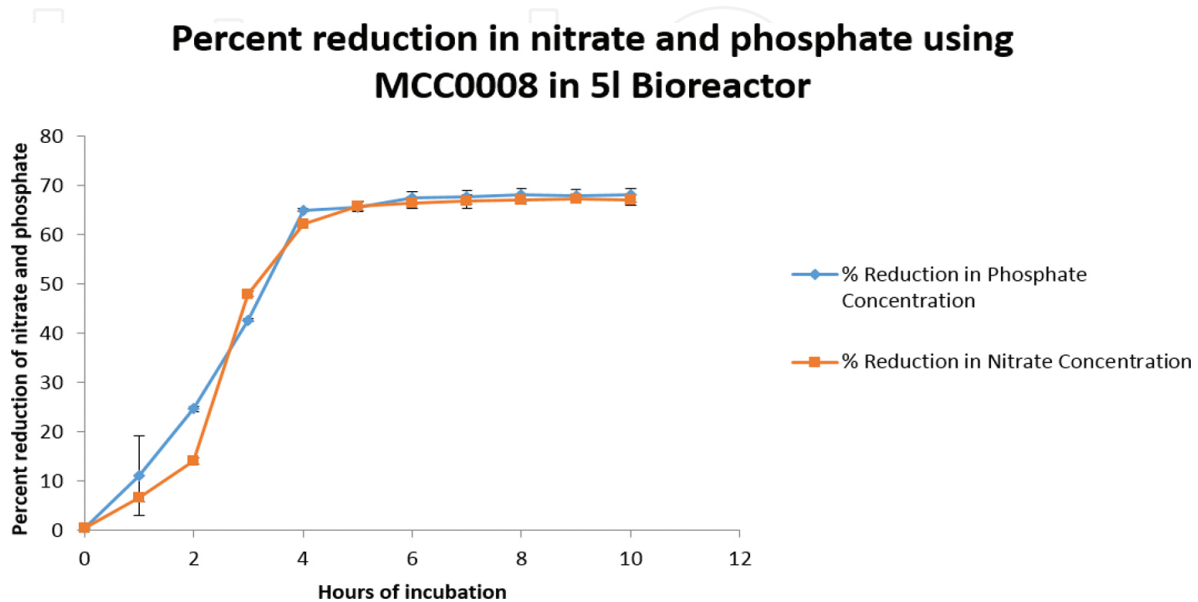


Figure 7. Percent reduction in nitrate and phosphate concentration with time using MCC0008 in 5 L suspended bioreactor.

4. Immobilization and acclimatization in a packed bed bioreactor

Fixed packed bed configuration has high surface area to volume ratio, thereby increasing the microbial density and improving the conditions necessary for nutrient removal. Biofilm-based reactors also have the advantage over other types of bioreactors with respect to ease of operation, high-density accumulation of microbe, resistance of the system to environmental stress [13] and do not require any additional measure to retain biomass in culture [14]. Rotating biological contractors (RBC), trickling filters and biofilm membrane bioreactor are some of the widely used biofilm-based bioreactor. Thus, in order to make the system more cost-effective along with better nutrient sequestration rate, the abilities of the isolate were further exploited. In order to exploit these biofilm forming, nitrate, and phosphate sequestration abilities, a reactor packed with suitable matrix with a fixed bed was developed. The bioreactor was designed of glass with steel mesh as immobilization matrix (Figure 8). The isolate could bind equally well to steel and plastic. The total capacity of the bioreactor was 9 L with a working volume of 5 L post-filling up with steel matrix up to sixty percent capacity. The steel mesh acted as the matrix for the formation of MCC0008 biofilm. Ports were designed at different heights of the bioreactor as shown in the Figure 8.

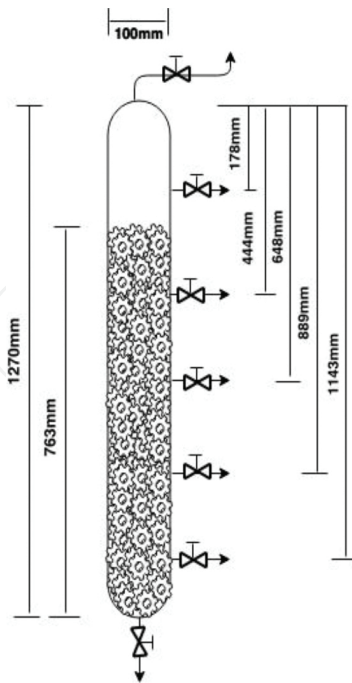


Figure 8. Schematic diagram of 9 L packed bed bioreactor.

The graphical representation shows the initial acclimatization period for proper biofilm development. The initial rise and fall in the performance correlate well with the biofilm character of slough off and growth to achieve stability. It required about 30 loadings to attain stability. After the 39th loading, approximately full nitrate reduction was obtained in one hour only in nitrate broth which was retained for more than 90 days (Figure 9a).

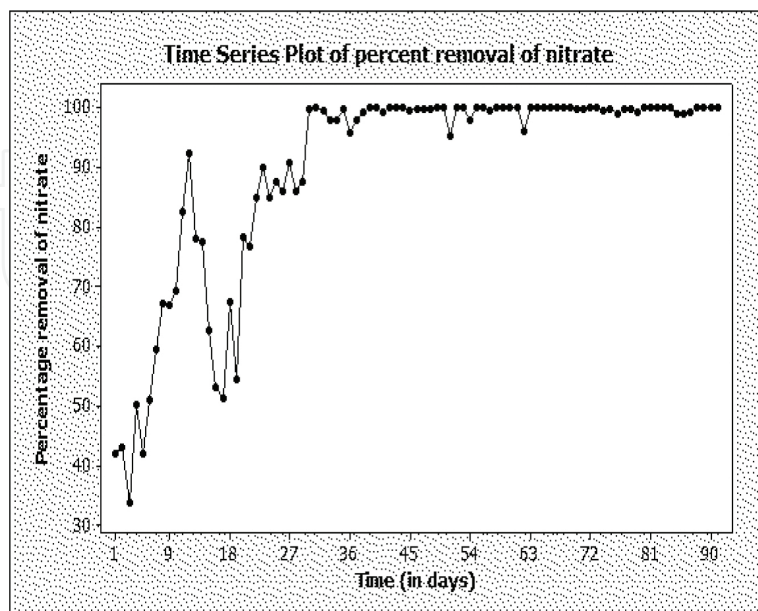


Figure 9a. Performance in terms of nitrate removal plotted as a time series.

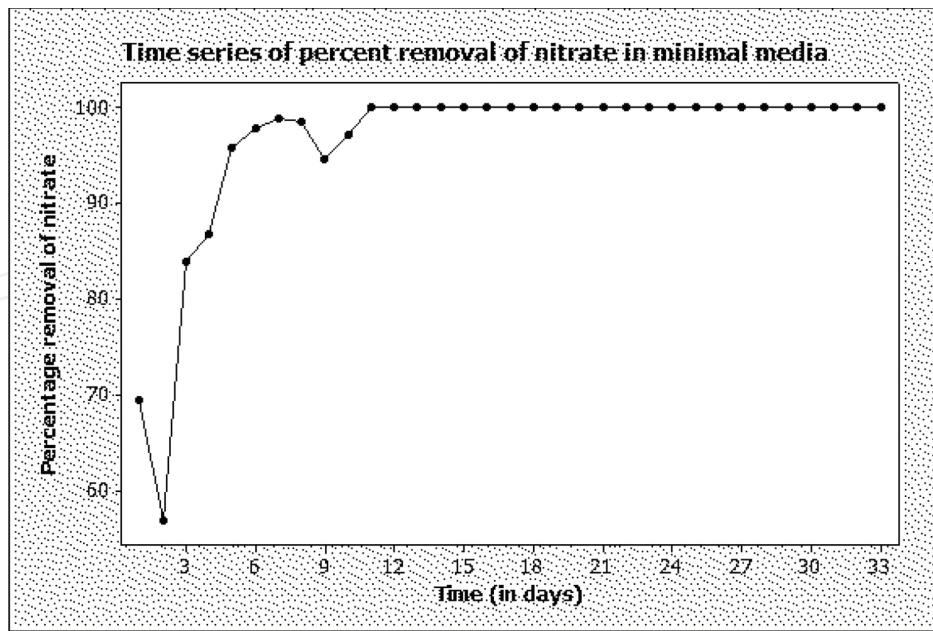


Figure 9b. Performance in terms of nitrate removal in minimal medium with time.

After stable performance of the bioreactor in enriched media, next the performance of the reactor was monitored in minimal media (**Figure 9b**). This was done in order to acclimatize the reactor to minimal conditions before exposure to waste water. It contained 495ppm nitrate and 1% glycerol.

The biofilm was observed to be dense with thick layer of polysaccharide during environmental scanning electron microscopy (**Figure 10**).

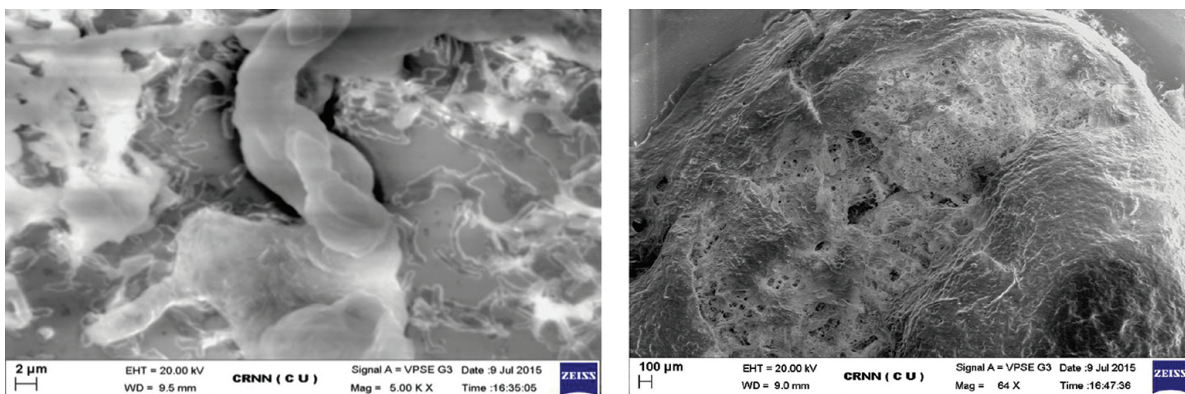


Figure 10. Environmental scanning electron micrograph taken using Zeiss EVO-MA 10 of the biofilm on the inert matrix of a packed bed bioreactor.

Post-acclimatization of the biofilm to minimal media, non-radioactive wastewater was charged. The dynamics of nitrate removal in batch mode is reflected in **Figure 11**. Since the isolate is from a consortium acclimatized to radioactive waste water, it is expected to show similar performance with low-level radioactive waste.

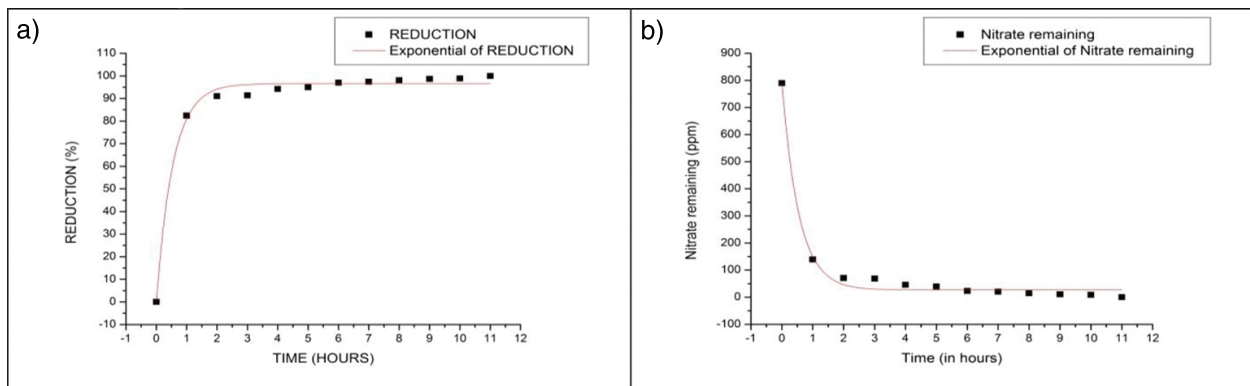


Figure 11. Kinetics of nitrate removal from waste water in batch mode. (a) Nitrate reduction kinetics following nonlinear curve fit (exponential). (b) Kinetics of remaining nitrate in the medium from 0 h (time of charging).

The equation, statistics, summary, and ANOVA for nitrate reduction kinetics (depicted in **Figure 11a**) are as follows:

$$y = y_0 + A * e^{(R0*x)}$$

where y = % Reduction, y_0 = initial nitrate concentration, x = time (in hours).

Statistics:

	Reduction
Number of points	12
Degrees of freedom	9
Reduced Chi squarer	7.39081
Residual sum of squares	66.51727
Adj. R-square	0.99046
Fit status	Succeeded(100)

The equation, statistics, summary, and ANOVA for remaining nitrate in the medium with time (depicted in **Figure 11b**) are as follows:

$$y = y_0 + A * e^{(R0*x)}$$

where y = Remaining nitrate in the medium, y_0 = initial nitrate concentration, x = time (in hours).

Complete nitrate removal from wastewater took place in 11 h. The longer retention time for waste water treatment as compared to that in minimal media in terms of nitrate removal may

be due to the presence of other contaminants to which the biofilm is sensitive. Multivariate analysis using response surface methodology revealed higher nitrate removal at higher initial concentration of nitrate with little effect of the flow rate (within the range tested) on the system performance (**Figure 12**).

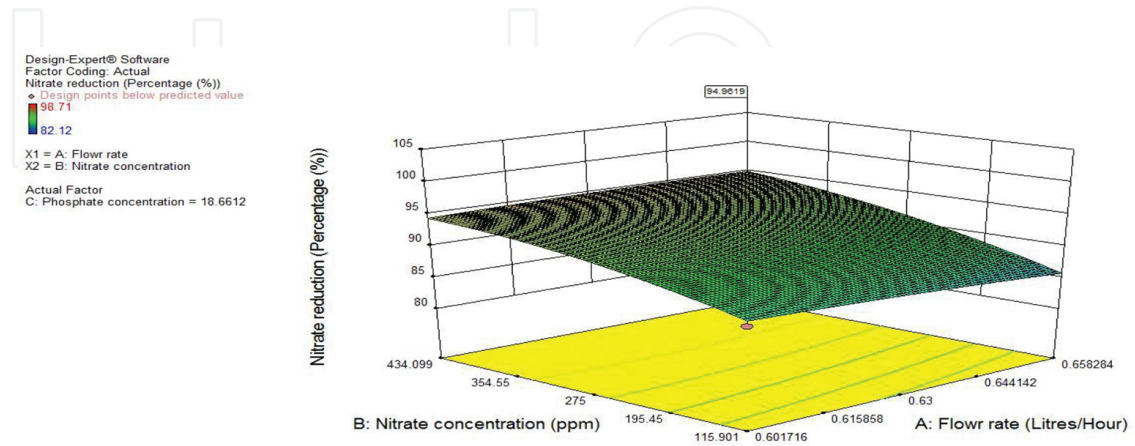


Figure 12. The figure shows the response of nitrate concentration and flow rate on nitrate reduction in the bioreactor.

Response	1 Nitrate reduction					
ANOVA for response surface quadratic model						
Analysis of variance table [Partial sum of squares— Type III]						
Source	Sum of Squares	df	Mean Square	F Value	p-value Prob > F	
Model	279.17	9	31.02	17.36	0.0029	Significant
A-Flow rate	14.96	1	14.96	8.37	0.0340	
B-Nitrate concentration	76.14	1	76.14	42.61	0.0013	
C-Phosphate concentration	1.25	1	1.25	0.70	0.4414	
AB	0.93	1	0.93	0.52	0.5034	
AC	4.56	1	4.56	2.55	0.1711	
BC	0.39	1	0.39	0.22	0.6586	
A2	0.42	1	0.42	0.24	0.6477	
B2	12.37	1	12.37	6.92	0.0465	
C2	14.61	1	14.61	8.18	0.0354	
Residual	8.93	5	1.79			
Lack of fit	7.84	1	7.84	28.59	0.0059	Significant
Pure error	1.10	4	0.27			
Cor total	288.11	14				

Std. dev.	1.34	R-squared	0.9690
Mean	92.69	Adj R-squared	0.9132
C.V. %	1.44	Pred R-squared	-1.9466
PRESS	848.93	Adeq precision	15.118

Factor	Coefficient		Standard		95% CI		VIF
	Estimate	df	Error	Low	High		
Intercept	94.22	1	0.58	92.74	95.70		
A-Flow rate	-1.93	1	0.67	-3.65	-0.22	2.00	
B-Nitrate concentration	4.36	1	0.67	2.64	6.08	2.00	
C-Phosphate concentration	0.56	1	0.67	-1.16	2.28	2.00	
AB	0.68	1	0.95	-1.75	3.11	2.00	
AC	-1.51	1	0.95	-3.94	0.92	2.00	
BC	0.44	1	0.95	-1.99	2.87	2.00	
A^2	-0.23	1	0.48	-1.47	1.00	1.00	
B^2	-1.27	1	0.48	-2.50	-0.029	1.00	
C^2	-1.38	1	0.48	-2.61	-0.14	1.00	

The final equations obtained through RSM-based optimization are as follows:

$$\begin{aligned} \text{Nitrate reduction} = & -81.1 + 424.3 * \text{Flow rate} - 0.049 * \text{Nitrate concentration} + 4.74 \\ & * \text{phosphate concentration} + 0.15 * \text{Flow rate} * \text{Nitrate concentration} - 6.04 * \text{Flow} \\ & \text{rate} * \text{Phosphate concentration} + 3.13e^{-004} * \text{Nitrate concentration} * \text{Phosphate} \\ & \text{concentration} - 292.25 * \text{Flow rate}^2 - 5.002e^{-005} * \text{Nitrate concentration}^2 - 0.018 * \\ & \text{Phosphate concentration}^2 \end{aligned}$$

The packed bed bioreactor system could treat waste water optimally removing 94.46% nitrate within 11 h in batch mode while 8 h in continuous mode from waste water containing 275 ppm of nitrate at 0.63 L/h flow rate.

5. Application as biofertilizer

Singh et al. [15] conducted experiments using *Advenella species* (PB-05, PB-06, and PB-10) and *Cellulosimicrobium* sp. PB-09 to analyze the IAA production, HCN production, ammonia production, and phosphate solubilization and correlated the results to the isolates' capability to promote plant growth. For them the isolates positively affected all characteristics except HCN production [15]. Since the isolate MCC0008 could accumulate both nitrate and phosphate simultaneously and also produce phosphatase, its effect on plant growth promotion was checked in case of mung bean (*Vigna radiate* var Samrat). **Table 2** representing the germination

percentage, germination index, and vigor index for Mung bean (*Vigna radiata*) seeds with and without treatment with isolate (soil and seed application) revealed better germination upon soil application. It was expected since the isolate produces plant growth hormones.

Sample	Control	MCC0008 (coated)	MCC0008 (soil)
Germination percentage	74.074	83.333	87.037
Germination index	39.772 ± 9.39	62.298 ± 12.234	75.313 ± 9.44
Vigor index	1639.056	2390.688	2006.801

Table 2. The table shows the germination parameters in case of mung bean upon application of MCC0008.

Soil application gave better result, and so further experiments were conducted by sowing soaked seeds, followed by soil application of the isolate. The germination in the presence of antifungal agent (Saaf) was better upon application of the isolate to soil.

Elements	MCC0008	Changes in %
		Chemical
Zn	16.04	-7.99
Fe	2.84	-7.20
Mn	14.49	7.08
Cu	25.41	8.97
P	12.82	-66.60
K	4.39	-19.16
S	12.57	-26.24
Ca	5.59	-12.59

The control was taken as reference and that for biofertilizer and chemical fertilizer was calculated accordingly.

Table 3. Chance in elemental content of seed grown without fertilizer (control), with chemical fertilizer and with biofertilizer.

Pot trial and field trial were carried out. For field trial, randomized block design with four replicates was carried out. The sowing was done in the north–south orientation. The seeds' post-germination was subjected to thinning such that each 1 m² area contained a total of 40 plants (4 rows of 10 plants each). The inoculum for the germination trial was 4.2 × 10⁶ cells per 125 gm soil in a thermo coal glass/germination tray, 1.39 × 10⁷ cells per 8 kgs soil in each pot and 3.68 × 10⁹ cells per 1 m² plot for field trial. The yield per hectare of land was calculated for the consortium when compared with control (without fertilizer) and chemical fertilizer application. The yield per hectare for control, MCC0008 application, and chemical fertilizer application was 1277.5 kg, 1974.5 kg, and 1685 kg, respectively. The elemental content improved post-application as compared to control as measured through EDXRF analysis

(Table 3). This shows that not only the yield improves as compared to chemical fertilizer but also the elemental content was better as compared to control as well as chemical treatment in MCC0008-treated seeds. The data revealed that upon treatment with MCC0008, there was desirable change in the nutritional quality parameters. There was increase in energy value (4.3%), total carbohydrate (4.5%), total sugar (0%), total dietary fiber (4.5%), protein (4.9%) content while a decrease in moisture content (23.4%), total ash (6.4%), and crude fat (7.5%). The decrease in moisture would ensure better storage of the grains, decrease in ash content means less non-utilizable component, while decrease in fat improves the quality further.

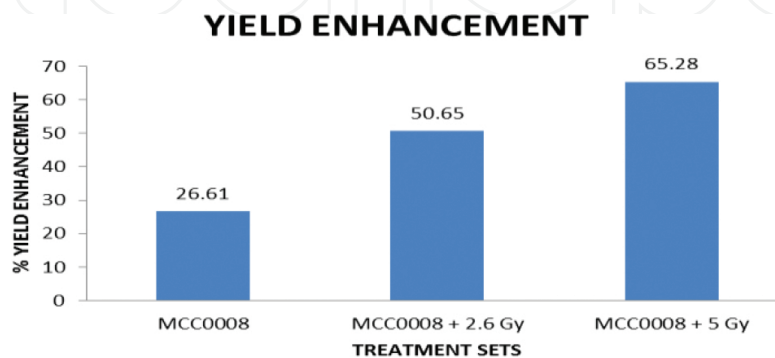


Figure 13. Yield enhancement of mung bean in the presence of biofertilizer with and without gamma irradiation.

According to the previous reports, gamma irradiation of seeds brings about faster germination [16–18]. This is due to increased levels of transcription. The antinutrient as well as elemental levels following irradiation (presowing) is also reported to be lower. Thus, a combined effect of low-dose gamma irradiation of mung bean seeds along with biofertilizer application was tested. The effect of combined application of low-dose gamma irradiation (2.6 Gray and 5 Gray) on germination, yield enhancement, and elemental content of mung bean seeds were tested. The cell structure and viability of the irradiated seeds were studied following ESEM analysis and microtomy using standard techniques. There was mild improvement in germination following irradiation at 5 Gray while significant yield enhancements in irradiated seeds as shown in the Figure 13.

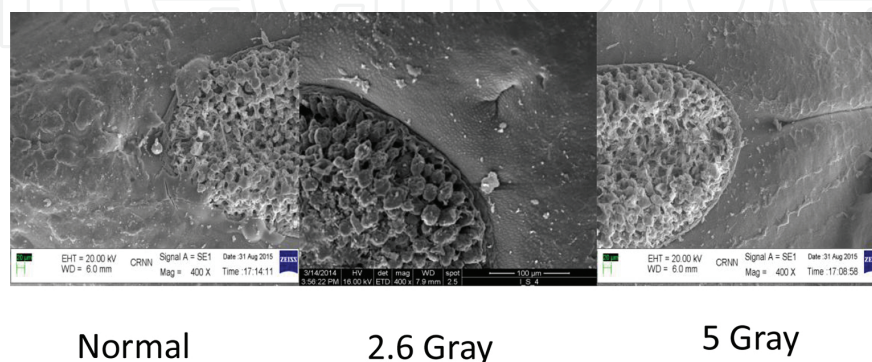


Figure 14a. ESEM image of control and irradiated seeds showing part of the seed coat and hilum.

In order to explore the reason behind improved germination, detailed analysis of seed structure and hilum morphology was carried out using ESEM as shown in **Figure 14a** and **b**.

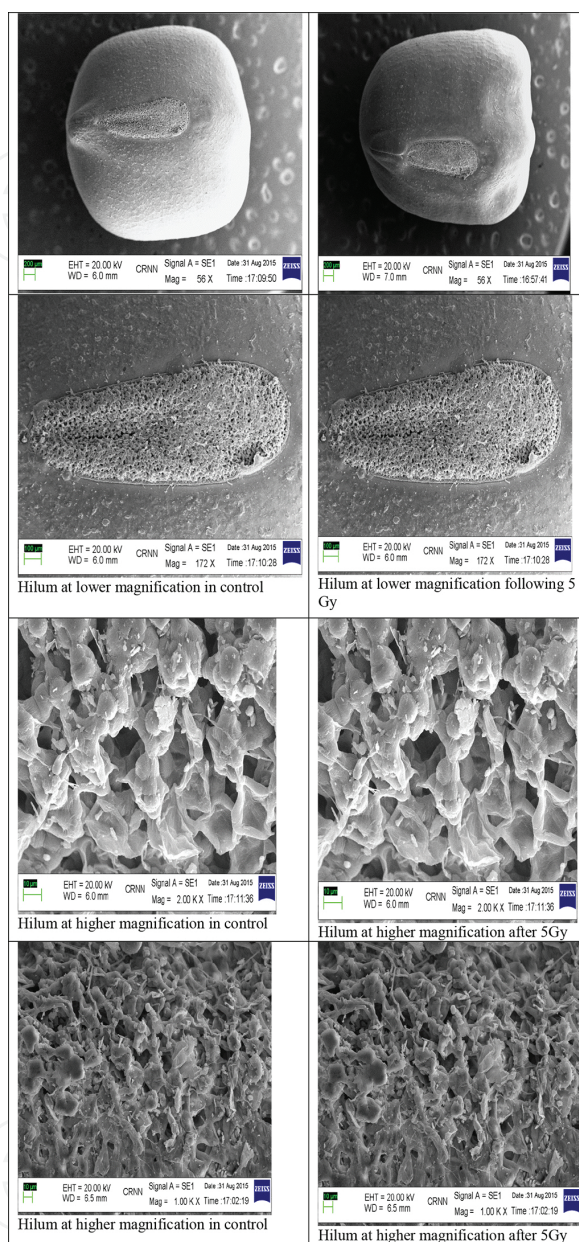


Figure 14b. ESEM analysis seed coat and the hilum of un-irradiated and irradiated seeds.

However, this depth of analysis could reveal just dehydration and nothing beyond that. Dehydration is expected to delay germination, while here we observe faster germination. Hence, there must be some other phenomenon which is induced during irradiation. Since germination is initiated through hilum and it is the point of contact for imbibition of water, further analysis with conventional microtomy was carried out. It revealed loosening of the compact arrangement of protein sheets with starch granules upon irradiation (**Figure 15**). Since irradiation might inactivate the germplasm hence viability staining was carried out for the

same set, it was revealed that the vitality of the seeds was maintained for the irradiated seeds within the range tested. Hence, low-dose gamma irradiation does not destroy the seed but makes the hilum loose to enable better uptake of water and nutrients and hence faster germination and enhanced yield. Further analysis at the transcription level will be required for better understanding of the phenomenon.

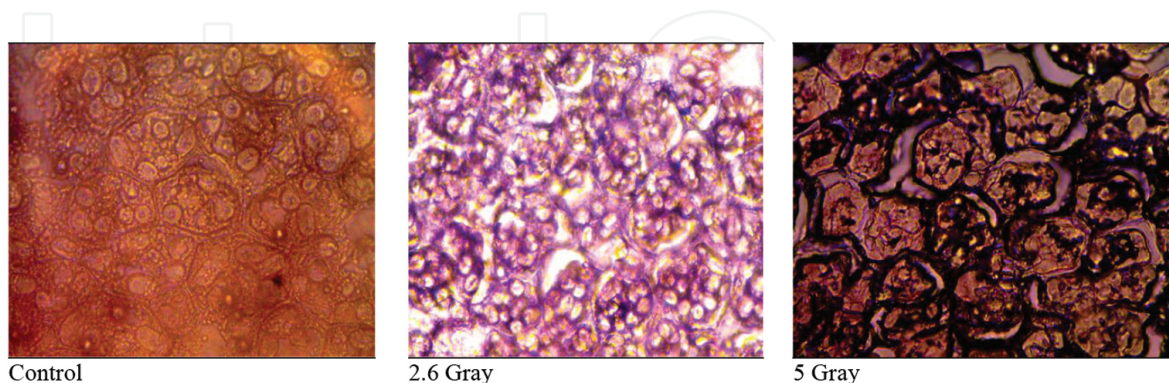


Figure 15. Microtomy images of hilum at 40× magnification of Dewinter Trinacular Microscope (New Crown) showing disintegration of compact protein sheets with irradiation.

The application of this strain as biofertilizer to enhance yield while maintaining nutritional quality of the grain and soil fertility has been filed as patent application in India [19]. To protect the intellectual property associated with this discovery, a PCT has also been filed [19].

6. Bioinformatics-based strain identification

The genus “*Bacillus*” has a long history of importance, both from an economic point of view and as a source of experimental microorganisms. Bacteria of the genus *Acinetobacter* were originally thought to be the major PAOs (polyphosphate accumulating organism). The pure isolate of nitrate accumulating *Bacillus* sp. MCC0008 showed potential for waste water treatment as well as biofertilizer application, hence of immense commercial importance. Knowing the identity of the strain becomes essential for better understanding of the system. This study was undertaken to decipher its species identity as per standard procedure [20] while exploring its underlying phenomenon of nitrate and phosphate accumulation. ANI (Average Nucleotide Identity) was calculated using ANI calculator for this strain with respect to the type strains of *Bacillus cereus*, *Bacillus thuringiensis*, and *Bacillus anthracis*. The ANI calculator estimates the average nucleotide identity using both best hits (one-way ANI) and reciprocal best hits (two-way ANI) between two genomic datasets [21]. Inter-genomic distances between this strain and its closest neighbors were determined using Version 2.0 of the DSMZ Genome-To-Genome Distance calculator, an *insilico* version of DNA-DNA hybridization [20]. The draft genome of each isolate was compared to the genome sequence of the type strains of *Bacillus cereus*, *Bacillus thuringiensis*, and *Bacillus anthracis* using dot plot analysis through a genomic similarity search tool, YASS [20, 22], to understand the similarities between the isolates over the length of their genomes. The contigs were uploaded to the Rapid Annotation using

Subsystems Technology (RAST) server, which is a fully automated service for annotating bacterial and archaeal genomes and provides high-quality annotation for these genomes across the phylogenetic tree. The annotated genomes in the seed viewer depicted the metabolic patterns for the strain and the four reference *Bacillus* strains. The gene arrangements on each chromosomal segment were compared for the strain with that of the other *Bacillus* sp. for phosphate metabolism as per earlier studies [20]. Furthermore, metabolic pathway reconstruction was performed using the Kyoto Encyclopedia of Genes and Genomes (KEGG) database through RAST. The genomes were compared in terms of the number of genes involved in different metabolic pathways and in phosphate metabolism as compared with the type strains.

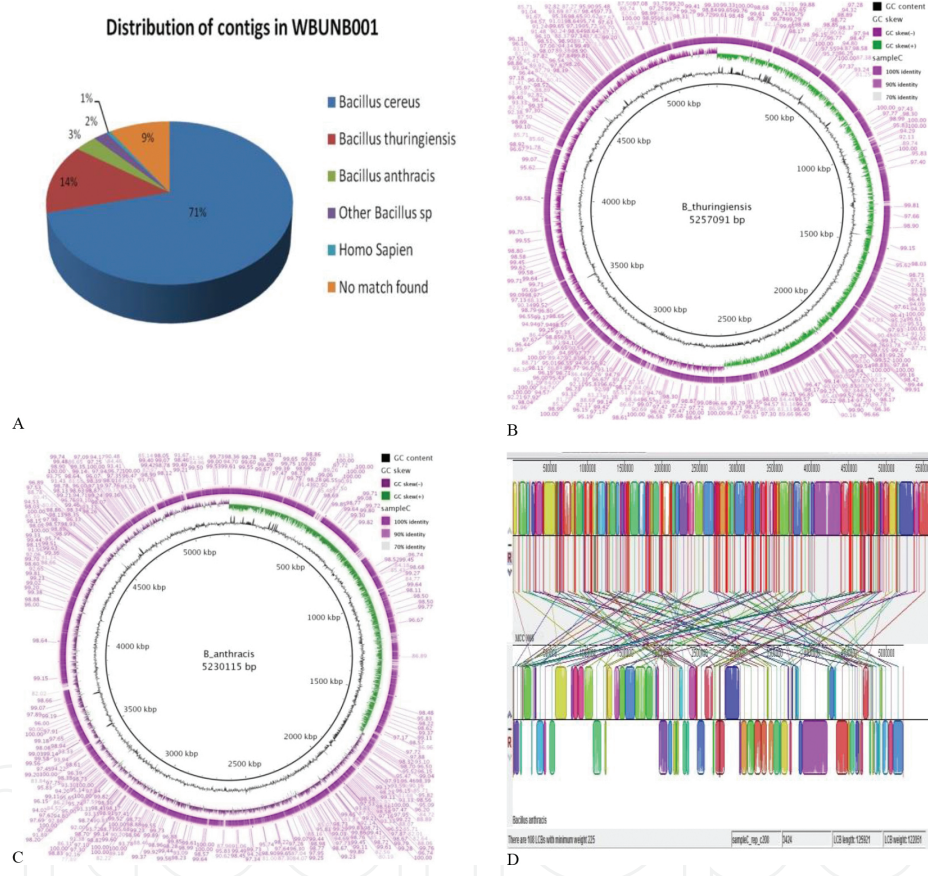


Figure 16. Genomic comparison of the draft genome of MCC0008 (also named WBUNB001) with other members of *Bacillus* species. **(A)** Pie chart of the data generated following blast analysis of the contigs revealing maximum similarity with different organisms. Maximum similarity of major portion of the contigs is with *Bacillus cereus*. **(B)** Represents the comparison of the genome of MCC0008 with *Bacillus thuringiensis*. The graphs depicted gene transfer within the genome (GC content) while the GC skew data which should be 50% positive and 50% negative under ideal condition showed 45–50% +ve with *Bacillus thuringiensis*. **(C)**. Represents the comparison of the genome of MCC0008 with *Bacillus anthracis*. The graphs depicted gene transfer within the genome (GC content) while the GC skew data which should be 50% positive and 50% negative under ideal condition showed about 30%+ve with *Bacillus anthracis*. The gap in the genome sequence was also revealed through this analysis. This analysis also revealed maximum identity with *Bacillus cereus* at the nucleotide level. **(D)** Mauve analysis to determine genome rearrangement when compared with *Bacillus anthracis*. There is extensive rearrangement in all three cases emphasizing the isolate to be a novel species different from these three type strains of *Bacillus* sp.

The phylogenetic analysis of the novel strain was done with its closest neighbors using the 16SrRNA sequence as well as using seven housekeeping genes, namely RNA polymerase B (rpo B), gyrase B subunit (gyrB), pyruvate carboxylase A (pyc A), malate dehydrogenase (mdh), rod shape determining protein (MreB), DNA mismatch repair protein (MutS), and transcription regulator (pIcR). The software used was MEGA (Molecular Evolutionary Genetics Analysis) Version 6.0. MEGA is an integrated tool which is used for constructing sequence alignment, inferring phylogenetic trees, estimating divergence times, mining online databases, estimating rates of molecular evolution, inferring ancestral sequences, and testing evolutionary hypotheses. MEGA is used by biologists in a large number of laboratories for reconstructing the evolutionary histories of species and inferring the extent and nature of the selective forces shaping the evolution of genes and species.

The draft genome sequence of *Bacillus* sp. MCC0008 had a total number of assembled reads of 1,740,538, with 331 contigs (43 × coverage), in which 315 were large with 35.1% G + C content. A total of 307Mb were sequenced with 202Mb having quality values >20 [11]. Average nucleotide identity and phylogenetic analysis revealed that *Bacillus* sp. MCC0008 is closest to *Bacillus anthracis* while FAME (Fatty Acid Methyl Esters), PLFA (Phospholipid-Derived Fatty Acids), BLAST (Basic Local Alignment Search Tool), Dot plot and BRIG (BLAST Ring Image Generator) analysis and partial 16SrDNA revealed maximum identity with *Bacillus cereus*. However, MAUVE analysis performed on the draft genome of MCC0008 (GenBank Accession Number: ANAU00000000) with the type strains of *Bacillus cereus*, *Bacillus thuringiensis*, and *Bacillus anthracis* revealed extensive genomic rearrangements while RAST analysis revealed 40% subsystem coverage whereas remaining 60% did not have identity with any known sequence stretch. From the combined interpretation, it is apparent that the strain under investigation is novel species of genus *Bacillus* (**Figure 16**).

House-keeping genes	Closest neighbor
DNA gyrase subunit B	<i>Bacillus anthracis</i> str Ames and <i>Bacillus anthracis</i> str Sterne
DNA-directed RNA polymerase beta subunit	<i>Bacillus thuringiensis</i> serovar konkukian str 97-27
Malate dehydrogenase	<i>Bacillus anthracis</i> str A1055
DNA mismatch repair protein mutS	<i>Bacillus anthracis</i> str Ames and <i>Bacillus anthracis</i> str Sterne
Phosphatidylinositol specific phospholipase C	All the strains of <i>Bacillus anthracis</i>
Rod shape determining protein MreB	<i>Bacillus anthracis</i> str Ames and <i>Bacillus anthracis</i> str Sterne
Pyruvate carboxyl transferase	<i>Bacillus thuringiensis</i> str. Al Hakam
Partial 16S rRNA	<i>Bacillus cereus</i>

Table 4. Closed neighbor of MCC0008 in case of the house-keeping genes.

DNA–DNA hybridization which calculate the inter-genomic distances between the strains with the score of >70% indicates the same species. The strain was compared with the type strains of *Bacillus anthracis* (Ba), *Bacillus thuringiensis* (Bt), and *Bacillus cereus* (Bc) revealing a value of $81.8 \pm 2.72\%$, $79 \pm 2.82\%$, and $61.3 \pm 2.83\%$ respectively. Hence *Bacillus* sp. MCC0008

was closest to *Bacillus anthracis* (Ba), followed by *Bacillus thuringiensis* and had the least identity with *Bacillus cereus*. The phylogenetic analysis of the different housekeeping genes at the nucleotide sequence level showed similarity with different species of genus *Bacillus* as revealed in **Table 4** indicating it to be a novel species of genus *Bacillus*.

7. Phylogenetic analysis of putative protein

The nucleotide sequence stretches: ANAU01000001, ANAU01000016, ANAU01000020, ANAU01000033, ANAU01000036, ANAU01000046, ANAU01000052, ANAU01000062, and ANAU010000274— each containing several genes – from the draft genome of MCC0008 [11] were translated in MEGA6 [23] using the standard genetic code. The protein sequences generated from these stretches were submitted to HAMAP [24], Interproscan [25, 26], EMBL-Fasta [26, 27], Prositescan [26, 27], and NPSA blast [28] for predicting their functions. The largest amino acid sequence stretch derived from ANAU01000036 was divided into parts, and the protein blast search of NCBI [29] was used to decipher the function of its individual proteins. The consensus predictions from the tools used, were selected for further detailed analysis. Each of the prediction was verified by scanning the proteins for function specific sequence signatures, using the Scanprosite [30, 31] tool. Alternatively, conserved patterns were identified from the HAMAP seed alignment [24] and uniprot protein cluster – UniRef [32] of the said functional protein category.

Nucleotide sequence stretch of MCC0008	Putative protein	Closest species	Prosites entry	HAMAP entry	UniRef entry	Sequence motif in MCC0008
ANAU01000001	Malate synthase	<i>Bacillus cereus</i>	PS00510			KDHSAGLNCGRWDYIF
ANAU01000001	NAD kinase	<i>Bacillus anthracis</i>		MF_00361		GGDG
ANAU01000001	FabH	<i>Bacillus cereus</i>		MF_01815		AACAGF
ANAU01000001	ATP dependent helicase	<i>Bacillus cereus</i>		MF_01452		LIA
ANAU01000001	Peptide ABC transporter permease	<i>Bacillus anthracis</i>	PS50928			TRVSLYIALLAAIDLIVGVAYGGISAF
ANAU01000001	spx transcription regulator	<i>Bacillus thuringiensis</i>		MF_01132		IDEKRLQVGY, SCTSC
ANAU01000016	Quinone oxidoreductase	<i>Bacillus cereus</i>	PS01162			VLIHAAAGGIGTT
ANAU01000020	Zinc containing alcohol dehydrogenase	<i>Bacillus thuringiensis</i>	PS00059			GHEFSGEV
ANAU01000020	Transaldolase	<i>Bacillus cereus</i>	PS01054			GVTTPSLV
ANAU01000020	Phosphate uptake ABC transporter permease	<i>Bacillus anthracis</i>	PS50928			RLCIETMASLPSIVVGLFGLLVFVTMTGW

Nucleotide sequence stretch of MCC0008	Putative protein	Closest species	Prosite entry	HAMAP entry	UniRef entry	Sequence motif in MCC0008
ANAU01000020	FAD dependent oxidoreductase	<i>Bacillus cereus</i>	PS00862			IRVVGSGH
ANAU01000020	GerLA	<i>Bacillus anthracis</i>			UniRef50_Q93N70	PAMYVALVSYHQGLI
ANAU01000020	GerLB	<i>Bacillus cereus</i>			UniRef50_Q93N69	GTYLAW
ANAU01000033	Phosphoglycerate kinase	<i>Bacillus anthracis</i>	PS00111			RVDFNVP
ANAU01000033	Uvr domain A	<i>Bacillus cereus</i>	PS50151			EKTIAKMEAEMKEAAKALDFERAA
ANAU01000033	Uvr domain B	<i>Bacillus anthracis</i>	PS50151			EKTIAKMEAEMKEAAKALDFERAA
ANAU01000033	Central glycolytic genes regulator	<i>Bacillus thuringiensis</i>			UniRef90_A0RKS8	SASLGMT
ANAU01000033	Murein hydrolase export regulator	<i>Bacillus anthracis</i>			UniRef50_Q6HR39	TTVAIASD
ANAU01000033	Transcription regulator WhiA	<i>Bacillus anthracis</i>			UniRef50_O06975	TLKELGEMV
ANAU01000033	Autotransporter	<i>Bacillus cereus</i>	UniRef90_B7HGW2			LKREV
ANAU01000036	Acetyl ornithine deacetylase	<i>Bacillus cereus</i>			UniRef50_K0IAN5	YGRG
ANAU01000036	Acyl co-A dehydrogenase	<i>Bacillus anthracis</i>	PS00072			ALTEPNAGSDALS
ANAU01000036	Alpha beta hydrolase	<i>Bacillus cereus</i>		MF_00832		YDQR
ANAU01000036	Aminotransferase classIII	<i>Bacillus thuringiensis</i>	PS00600			FIADVMTGLGRTGAW
ANAU01000036	Aspartate semialdehyde dehydrogenase	<i>Bacillus cereus</i>	PS01103			MAATCVRVPVISGHS
ANAU01000036	ATPase AAA	<i>Bacillus cereus</i>			UniRef90_A0A0A0WLW6	NFNEN
ANAU01000036	Chloramphenicol acetyltransferase	<i>Bacillus cereus</i>			UniRef90_A0REA1	GETMG
ANAU01000036	Choloylglycine hydrolase	<i>Bacillus cereus</i>			UniRef90_Q81H11	GVNEHG
ANAU01000036	Citrate synthase	<i>Bacillus thuringiensis</i>	PS00480			GFGHRVY
ANAU01000036	Cold shock protein	<i>Bacillus anthracis</i>			UniRef50_Q45096	NLIFADTS
ANAU01000036	D-alanyl D-alanine carboxypeptidase	<i>Bacillus cereus</i>			UniRef90_Q6HBP6	SYAAGI
ANAU01000036	Diguanylate cyclase	<i>Bacillus cereus</i>			UniRef90_A0R9R1	NITLA
ANAU01000036	DNA binding protein	<i>Bacillus thuringiensis</i>	PS50943			LKTIREKEKLSLEKVSQLTGVSKTMIGQ
ANAU01000036	Glucokinase	<i>Bacillus cereus</i>			UniRef90_Q738U1	YQLFSRYVVD

Nucleotide sequence stretch of MCC0008	Putative protein	Closest species	Prosite entry	HAMAP entry	UniRef entry	Sequence motif in MCC0008
ANAU01000036	Membrane protein	<i>Bacillus cereus</i>			UniRef50_C3BJ03	LGITV
ANAU01000036	MFS transporter	<i>Bacillus cereus</i>	PS50850			MIRILAIVAFFVGLDSSLVAP
ANAU01000036	Multidrug ABC transporter	<i>Bacillus cereus</i>	PS50893			GPTGSGKTTIINLLTRFYD
ANAU01000036	NADH ubiquinone oxidoreductase	<i>Bacillus cereus</i>			UniRef90_Q81K10	ARGVYANA
ANAU01000036	Serine threonine protein kinase	<i>Bacillus cereus</i>	PS50011			IGMGSYGVTVV
ANAU01000036	Threonyl tRNA synthetase	<i>Bacillus cereus</i>		MF_00184		GFYYD, GAYWRGD
ANAU01000046	FenI	<i>Bacillus cereus</i>			UniRef90_Q6HIP8	NTTYKKHELRAVW
ANAU01000052	Nitrite/Nitrate response regulatory protein	<i>Bacillus cereus</i>	PS50110			SVLVVDDHVAVGLGKALIEKYDDMNVVVDST
ANAU01000052	ABC transporter	<i>Bacillus cereus</i>	PS50893			ILKQGETLGVVGTGSGKTTLVRQ
ANAU01000062	Non homologous End joining protein Ku	<i>Bacillus cereus</i>		MF_01875		WKG
ANAU01000062	Spore coat cotJA	<i>Bacillus cereus</i>			UniRef50_Q45536	HSPQDPCPPIGKKYY
ANAU010000274	Hypothetical protein					

Table 5. Comparison of contigs of MCC0008 with closest neighbor at the putative protein sequence level.

Hence from the combined interpretation it is concluded that due to extensive genomic rearrangement, *Bacillus* sp. MCC0008 has emerged to be a novel species.

The members of the Genus *Bacillus* comprising of *Bacillus cereus*, *Bacillus thuringiensis*, *Bacillus anthracis*, *Bacillus mycoides*, *Bacillus pseudomycoides*, and *Bacillus weihenstephanensis* [33–35], which share high degree of sequence similarity with MCC0008, were chosen for the functional annotation and the phylogenetic study of MCC0008. The protein sequences of the above group members, having the functions as predicted in MCC0008, were retrieved from the protein database of NCBI [36] as available. The sequences which could be acquired were aligned in MEGA6 [23] with the corresponding translated nucleotide stretches of MCC0008, using the clustalW program [37]. The protein weight matrix was set to BLOSUM [38]. The prosite motifs/ conserved patterns from HAMAP seed alignment/UniRef, pertaining to the relevant function, were searched in the alignments.

The consensus predictions for the translated nucleotide sequence stretches of the draft genome of MCC0008 are summarized in **Table 5**. The putative proteins showed sequence specific characteristics of the predicted functions, as validated through sequence motifs in the prosite database /HAMAP family profile/UniRef. The sequence alignments of the MCC0008 proteins

with the corresponding proteins of the Genus *Bacillus* and the presence of signatures from Prosite/HAMAP/UniRef therein brought out the sequence motifs of the group and the MCC0008 strain. The database entries along with the corresponding exact motif in MCC0008 are tabulated in **Table 5** again. The high degree of sequence similarity amongst MCC0008 and the members of Genus *Bacillus* resulted in these sharing the same protein sequence motif, with a few exceptions of diverging sequences of *Bacillus* sp. These hint that the isolated strain being reported could belong to the Genus *Bacillus* but not any of these known species. The phylogenetic trees computed for the different proteins show that in most of the cases, *Bacillus cereus*, *Bacillus anthracis*, and *Bacillus thuringiensis* gets clubbed with MCC0008, with *Bacillus mycoides*, *Bacillus pseudomycoides*, and *Bacillus weihenstephanensis* being clad out. The study indicates that MCC0008 is closest to *cereus*, *anthracis*, and *thuringiensis*. Further, *Bacillus cereus* emerges nearest to MCC0008 for ATP-dependent helicase, FabH, Malate synthase, Quinone oxidoreductase, FAD-dependent oxidoreductase, Transaldolase, GerLB, Uvr system domain A, Autotransporter, D-alanyl D-alanine carboxypeptidase, Glucokinase, NADH ubiquinone oxidoreductase, Membrane protein, Acetyl ornithine deacetylase, ATPase AAA, Serine threonine protein kinase, Diguanylate cyclase, Threonyl tRNA synthetase, Alpha beta hydrolase, Chloroamphenicol acetyltransferase, MFS transporter. Aspartate semialdehyde dehydrogenase, Choloylglycine hydrolase, Multidrug ABC transporter ATP binding protein, FenI, ABC transporter, Nitrite/nitrate response regulatory protein, End joining protein ku, spore coat protein CotJA. *Bacillus anthracis* on the other hand appears closest to MCC0008 for peptide ABC transporter permease, NAD kinase, Phosphate uptake ABC transporter, Phosphoglycerate kinase, GerLA, Uvr system domain B, Murein hydrolase export regulator, sporulation regulator WhiA, Acyl co-A dehydrogenase, Cold shock protein. Spx transcription regulator, Zn-containing alcohol dehydrogenase, Central glycolytic genes regulator, Amino-transferase class III, Citrate synthase, and DNA-binding protein show MCC0008 getting clubbed with *Bacillus thuringiensis*. The picture that emerges here is that the strain in question seems to be a novel species mostly toward *Bacillus cereus*, with traces of *Bacillus anthracis* and a dash of *Bacillus thuringiensis*. The probable novel strain MCC0008 which shares traits from *Bacillus cereus*, *Bacillus anthracis*, and *Bacillus thuringiensis* could have emerged from genetic rearrangements between these species of the *Bacillus* group. *Bacillus anthracis* which is not reported to be a phosphate accumulator appears nearest to MCC0008 for phosphate uptake ABC transporter permease and phosphoglycerate kinase. *Bacillus cereus* is in closest proximity to MCC0008 for the nitrite/nitrate response regulatory protein. It appears from these observations that the genetic components from *cereus*, *anthracis*, and *thuringiensis* have given rise to this novel strain which has acquired the unique property of phosphate and nitrate accumulation.

8. Transcriptome analysis (BioProject PRJNA222597)

From transcriptome analysis (**Figure 17** and **Table 6**), it is concluded that there is significant upregulation of sporulation genes, which can be due to the accumulation of poly-P in the bacterial cells [39]. The sporulation of *Bacillus* species initiates with the asymmetric division of

cellular compartment into two parts: the mother cell and the forespore. In the model organism *B. subtilis* (Bs), this process is temporally and spatially regulated by a set of sigma factors of RNA polymerase: the main vegetative sigma factor SigA and SigH in the pre-asymmetric division cell; SigE and SigK in the mother cell; and SigF and SigG in the forespore. The DNA-binding protein Spo0A is the master regulator for entry into sporulation in *B. subtilis* [40]. Further there is significant upregulation of serine protein kinase which also play a role in sporulation [41] and also there is upregulation of histidine kinase which also play a significant

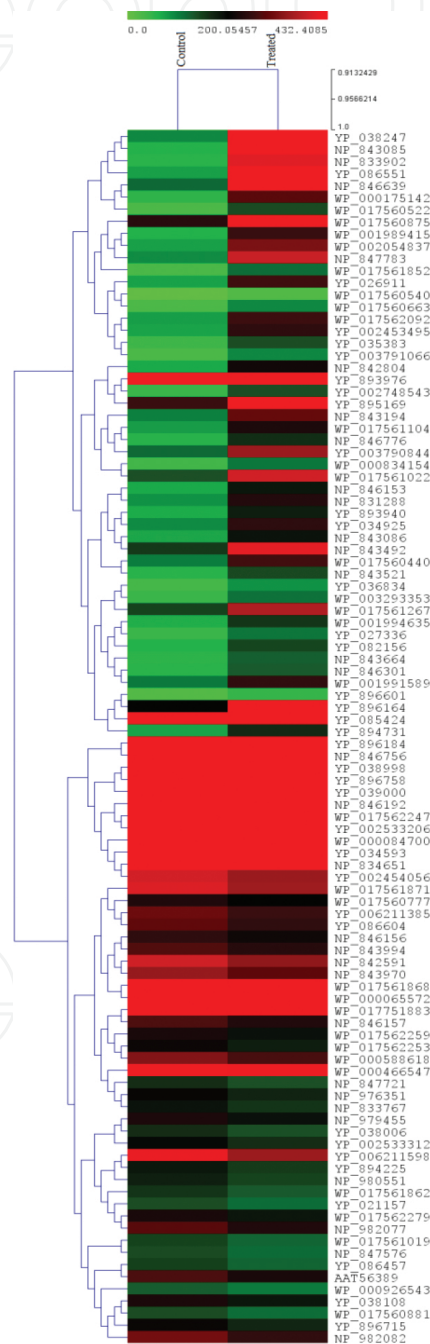


Figure 17. Heat map of top 100 differentially expressed transcript contigs in control and treated samples.

role in sporulation. The initiation of sporulation in *Bacillus subtilis* and most likely in aerobic *Bacillus* species in general is controlled by the phosphorelay signal transduction system [42]. The ultimate goal of the phosphorelay is to activate by phosphorylation the Spo0A transcription factor, which represses certain genes and promotes the transcription of a large number of genes for stationary-phase functions as well as sporulation [40, 43]. The signals that initiate the phosphorelay reactions are recognized and interpreted by several sensor histidine kinases [44–47]. The initiation of sporulation in *Bacillus subtilis* is controlled. *Bacillus* sp. MCC0008 synthesizes poly-p granules as revealed from the significant upregulation of phasin and also through polyphosphate staining and TEM analysis. Phosphorus (P) is an essential element for all cells as it is a component of, for example, DNA, RNA, and membrane lipids. The common phosphorus source is inorganic phosphate (P_i), which is taken up by bacteria either via secondary transporters or via ATP-driven ABC transporters. Extracellular phosphate esters can serve as an alternative P source. Phosphate esters are hydrolyzed by bacterial phosphatases and the resulting P_i imported into the cells. In addition, some bacteria utilize specific uptake systems for the transport of *sn*-glycerol-3-phosphate as organophosphate. The intracellular P_i is assimilated into cellular metabolites by reactions such as F1F0-ATP synthase or glyceraldehyde-3-phosphate dehydrogenase. Moreover, polyphosphate can be formed as a readily available intracellular P_i source. From the transcriptome analysis, it is revealed that there is downregulation of glyceraldehyde-3-phosphate dehydrogenase; hence, there is no assimilation of phosphate in the form of poly-P.

For nitrate accumulation, it is hypothesized that the nitrate accumulation occurs due to electrochemical gradient (Δp) [48]. In plants, typically vacuolar-type H^+ ATPases and H^+ pyrophosphatases (HPPases) catalyze a proton translocation over endomembranes to generate a Δp for solute transport and likely also nitrate transport [49]. Vacuolar-type ATPases also occur in plasma membranes of some Archaea, but they are rarely encountered in Bacteria [50, 51]. A vacuolar H_p -pyrophosphatase (*hppA*) and an uncommon Ca^{2+} translocating ATPase, may also contribute to generation of a $\Delta p/\Delta Ph$ [52]. From transcriptome analysis it is revealed that there is 3.95-fold change in cation-transporting ATPase, which can be responsible for electrochemical gradient and nitrate accumulation.

Genes	Protein encoded	Fold Change	log2Fold Change	Function
BCK_14255	Stage III sporulation protein AH	12.53	3.65	Involved in forespore engulfment
BCK_05395	Serine protein kinase	11.43	3.51	Kinase enzyme that phosphorylates the OH group of serine
BCK_14250	Stage III sporulation protein AG	10.31	3.37	Sporulation resulting in formation of a cellular spore
BCK_17375	Hypothetical	12.84	3.68	Unknown

Genes	Protein encoded	Fold Change	log2Fold Change	Function
	protein			
BCK_14245	Stage III sporulation protein AF	8.94	3.16	Leading to endospore formation
BCK_08950	Stage II sporulation protein	8.80	3.14	Sporulation resulting in formation of cellular spore
BCK_17370	Uncharacterized protein	8.08	3.01	Unknown
BCK_23315	Uncharacterized protein	9.89	3.31	Unknown
BCK_12895	Stage VI sporulation protein D	6.18	2.63	Required for assembly of a normal spore coat. May be a component of the innermost layer of the spore coat that aids in its adherence to the prespore.
BCK_02050	2-oxoglutarate dehydrogenase E1 component	5.89	2.56	The 2-oxoglutarate dehydrogenase complex catalyzes the overall conversion of 2-oxoglutarate to succinyl-CoA and CO ₂ . It contains multiple copies of three enzymatic components: 2-oxoglutarate dehydrogenase (E1), dihydrolipoamide succinyltransferase (E2) and lipoamide dehydrogenase (E3).
BCK_02290	Uncharacterized protein	5.81	2.54	Unknown
BCK_08430	Uncharacterized protein	5.84	2.55	Chromatin binding
BCK_17365	Hypothetical protein	5.67	2.50	Unknown
BCK_02225	Spore coat protein Z	5.92	2.57	Sporulation resulting in formation of a cellular spore
BCK_04810	Ribose import ATP-binding protein RbsA	5.07	2.34	Part of the ABC transporter complex RbsABCD involved in ribose import. Responsible for energy coupling to the transport system.
BCK_03255	Group-specific protein	6.24	2.64	Catalyses the phosphorylation of incoming sugar substrates concomitant with their translocation across

Genes	Protein encoded	Fold Change	log2Fold Change	Function
				the cell membrane
BCK_03260	Histidine kinase	4.02	2.01	Phosphorelay sensor kinase activity
BCK_04960	Amino acid ABC transporter ATP-binding protein	3.38	1.76	-

Table 6. Table showing fold change in expression of different genes during transcriptome analysis of MCC0008.

9. Conclusion

The isolate MCC0008 is an extracellular protease, amylase, lipase, catalase, oxidase, phosphatase, and DNase secreting strain which can form well-structured biofilm. It was isolated from a consortium developed from low-level radioactive waste treatment plant biomass. The strain is a novel species of genus *Bacillus* which falls within the group of *Bacillus cereus*. It could sequester nitrate within one hour from nitrate broth while took 11 hours to do the same from waste water under minimal condition in batch mode. This could be due to the antagonistic effect of the natural microflora of waste water or non-biological inhibitors. The well-developed biofilm ensured sustained performance of the system. The isolate during soil application retains phosphate and nitrate in the root zone ensuring better access to the plants. This was the reason behind approximately twofold and 1.2-fold yield enhancement as compared to no fertilizer and chemical fertilizer application respectively. Hence, microbial isolate from the low-level waste water treatment plant could help sequester essential plant growth nutrients from waste water. This would help reuse these nutrients while purify the water which in turn can be reused for agriculture and aquaculture, hence preventing wastage of potable water for non-potable application. This solution leads to environmental protection (prevention of eutrophication) and sustenance (organic farming).

Acknowledgements

The research was conducted using different funds from Government of India namely Department of Atomic Energy under the BRNS scheme (consortium isolation and characterization); Indian Council of Agricultural Research under the NFBSFARA (Biofertilizer application, pure strain isolation); Ministry of Human Resource and Development under the FAST scheme (strain characterization, development of packed bed reactor for waste water treatment), University Grant Commission-Department of Atomic Energy (testing pure isolate as biofertilizer with and without seed irradiation). The authors acknowledge the financial assistance

of all these granting agency. It also acknowledges the financial assistance of Department of Biotechnology, GOI for providing student fellowship The authors would like to thank Late Sourav Chakrorty, Arpan Pal and Abhishek Mitra for their technical assistance; Late Prof T K Das of Department of Anatomy, All India Institute of Medical Sciences, New Delhi, India for the TEM facility, Ms Nabanita Halder for extensively helping in the formatting of the manuscript.

Author details

Shaon Ray Chaudhuri^{1,4*}, Jaweria Sharmin⁴, Srimoyee Banerjee¹, U Jayakrishnan⁴, Amrita Saha⁵, Madhusmita Mishra⁴, Madhurima Ghosh⁴, Indranil Mukherjee⁵, Arpita Banerjee⁵, Kamlesh Jangid⁶, Mathummal Sudarshan⁷, Anindita Chakraborty⁷, Sourav Ghosh¹, Rajib Nath⁸, Maitreyi Banerjee⁹, Shiv Shankar Singh², Ajoy Krishna Saha³ and Ashoke Ranjan Thakur¹⁰

*Address all correspondence to: shaonraychaudhuri@tripurauniv.in;
shaon.raychaudhuri@gmail.com

1 Department of Microbiology, Tripura University, Tripura West, India

2 Department of Zoology, Tripura University, Tripura West, India

3 Department of Botany, Tripura University, Tripura West, India

4 Department of Biotechnology, Maulana Abul Kalam Azad University of Technology, Kolkata, India

5 Centre of Excellence in Environmental Technology and Management, Maulana Abul Kalam Azad University of Technology, Kolkata, India

6 Microbial Culture Collection, National Centre for Cell Science, Pune, Maharashtra, India

7 Laboratory of Trace Elements, Kolkata Centre, Kolkata, India

8 Bidhan Chandra Krishi Viswavidyalaya, Mohanpur, Nadia, West Bengal, India

9 West Bengal Council of Science and Technology, Bikash Bhavan, Kolkata, India

10 Formerly at West Bengal State University, Barasat, India

References

- [1] Sato T. The extraction of uranyl nitrate from nitric acid solutions by tributyl phosphate. *Journal of Inorganic and Nuclear Chemistry*. 1958; 6: 334–337. doi: 10.1016/0022-1902(58)80117-7.
- [2] Stas J, Dahdouh A, Shlewit H. Extraction of uranium (VI) from nitric acid and nitrate solutions by tributyl phosphate/kerosene periodica polytechnica. *Chemical Engineering*. 2005; 49: 3–18. <http://www.pp.bme.hu/ch/article/view/239>.
- [3] Ashbrook A, Lakshmanan V. Uranium purification. Canada: Eldorado Nuclear Ltd. 1986; 799–804.
- [4] Ray Chaudhuri S, Mukherjee I, Datta D, Chanda C, Krishna GP, Bhatt S, Datta P, Bhushan S, Ghosh S, Bhattacharya P, Thakur AR, Barat P. Developing tailor made microbial consortium for effluent remediation. In: Raheb Abdel Rahman, editor. *Nuclear materials*. InTech; 2016 (accepted). ISBN: 978-953-51-4676-6.
- [5] Mishra M, Jain S, Thakur AR, Ray Chaudhuri S. Microbial community in packed bed bioreactor involved in nitrate remediation from low level radioactive waste. *Journal of Basic Microbiology*. 2014; 54(3): 198–203. doi:10.1002/jobm.201200676.
- [6] DebRoy S, Das S, Ghosh S, Banerjee S, Chatterjee D, Bhattacharjee A, Mukherjee I, Ray Chaudhuri S. Isolation of nitrate and phosphate removing bacteria from various environmental sites. *OnLine Journal of Biological Science*. 2012; 12(2): 62–71. doi: 10.3844/ojbsci.2012.62.71.
- [7] Mussmann M, Hu FZ, Richter M, de Beer D, Preisler A, et al. Insights into the genome of large sulfur bacteria revealed by analysis of single filaments. *PLoS Bio*. 2007; 15: 1923–1937. doi:10.1371/journal.pbio.0050230.
- [8] Martin R, Soberon N, Vaneechoutte M, Florez AB, Vazquez F, et al. Characterization of indigenous vaginal lactobacillus from women as probiotic candidates. *International Microbiology*. 2008; 11: 261–266. doi:10.2436/20.1501.01.70.
- [9] Sayama M. Presence of nitrate-accumulating sulfur bacteria and their influence on nitrogen cycling in a shallow coastal marine sediment. *Applied and Environmental Microbiology*. 2001; 8: 3481–3487. doi:10.1128/AEM.67.8.3481.2001.
- [10] Hinck S, Neu TR, Lavik G, Mussmann M, Dirk de Beer, Jonkers HM. Physiological adaptation of a nitrate-storing *Beggiatoa* sp. to diel cycling in a phototrophic hypersaline mat. *Applied and Environmental Microbiology*. 2007; 73(21): 7013–7022. doi:10.1128/AEM.00548-07.
- [11] DebRoy S, Bhattacharjee A, Thakur AR, Ray Chaudhuri S. Draft genome sequence of the nitrate- and phosphate-accumulating *Bacillus* sp. strain MCC0008. *Genome Announcement*. 2013; 1: e00189–12. doi:10.1128/genomeA.00189-12.

- [12] Cataldo DA, Maroon M, Schrader LE, Youngs VL. Rapid colorimetric determination of nitrate in plant tissues by nitration of salicylic acid. *Communications in Soil Science & Plant Analysis*. 1975; 6: 71–80. doi:10.1080/00103627509366547.
- [13] Awan, Zhang, Zhong, Gao L, Chen X. Industrial wastewater treatment by using MBR (membrane bioreactor). Review Study, Huazhong University of Science and Technology. Wuhan, China, Scientific Research. 2015; 6: 584–598, doi:10.4236/jep.2015.66053.
- [14] Mark CM, Loosdrecht V, Heijnen SJ. Biofilm bioreactors for waste-water treatment. *Trends in Biotechnology*. 1993; 11(4): 117–121. doi:10.1016/0167-7799(93)90085-N.
- [15] Singh P, Kumar V, Agarwal S. Evaluation of phytase producing bacteria for their plant growth promoting activities. *International Journal of Microbiology*. 2014; 1–7. doi: 10.115/2014/426483.
- [16] Melki M, Marouani A. Effects of gamma rays irradiation on seed germination and growth of hard wheat. *Environmental Chemistry Letters*. 2010; 8: 307–310. doi:10.1007/s10311-009-0222-1.
- [17] Minisi AF, Fardous A, El-Mahrouk EM, Rida EM, Nasr MN. Effects of gamma radiation on germination, growth characteristics and morphological variations of *Moluccella laevis* L. *American-Eurasian Journal of Agricultural & Environment Science*. 2013; 13(5): 696–704. doi:10.5829/idosi.ajeaes.2013.13.05.1956.
- [18] Jan S, Parween T, Hamid R, Siddiqi TO, Mahmooduzzafar. Elemental, biochemical and essential oil modulation in developing seedlings of *Psoralea corylifolia* L. exposed to different presowing gamma irradiation treatment. *Journal of essential oil research*. 2015; 1–12. doi:10.1080/10412905.2015.1024890.
- [19] Ray Chaudhuri S. Method of improving elemental and nutritional content of plant seeds using bacillus strain MCC0008 as a biofertilizer. 1328/KOL/2013, dt 25th November 2013; PCT/IB2014/066010 dt 13th December 2014. (filed).
- [20] Ghoshal T, Ghosh S, Saha A, Haldar N, Thakur AR, Ray Chaudhuri S. Combination of conventional and in-silico approach for identifying industrially important isolates of *Aeromonas*. *OnLine Journal of Biological Sciences*. 2014; 14(2): 70–83. doi:10.3844/ojbsci.2014.70.83.
- [21] Goris J, Konstantinidis KT, Klappenbach JA, Coenye T, Vandamme P, Tiedje JM. DNA–DNA hybridization values and their relationship to whole-genome sequence similarities. *International Journal of Systematic and Evolutionary Microbiology*. 2007; 57(1): 81–91. doi:10.1099/ijs.0.64483-0.
- [22] Noe L, Kucherov G. YASS: enhancing the sensitivity of DNA similarity search. *Nucleic Acids Research*. 2005; 33: W540–W543. doi:10.1093/nar/gki478.
- [23] Tamura K, Stecher G, Peterson D, Filipski A, Kumar S. MEGA6: molecular evolutionary genetics analysis version 6. *Molecular Biology and Evolution*. 2013; 30: 2725–2729. doi: 10.1093/molbev/mst197.

- [24] Pedruzzi I, Rivoire C, Auchincloss AH, Coudert E, Keller G, Castro ED, Baratin D, Cuche BA, Bougueleret L, Poux S, Redaschi N, Xenarios I, Bridge A. HAMAP in 2015: updates to the protein family classification and annotation system. *Nucleic Acids Research*. 2015; 43: D1064–D1070. doi:10.1093/nar/gku1002.
- [25] Mitchell A, Chang HY, Daugherty L, Fraser M, Hunter S, Lopez R, McAnulla C, McMenamin C, Nuka G, Pesseat S, Sangrador-Vegas A, Scheremetjew M, Rato C, Yong SY, Bateman A, Punta M, Attwood TK., Sigrist JAC, Redaschi N, Rivoire C, Xenarios I, Kahn D, Guyot D, Bork P, Letunic I, Gough J, Oates M, Haft D, Huang H, Natale DA., Wu CH, Orengo C, Sillitoe I, Mi H, Thomas PD, Finn RD. The InterPro protein families database: the classification resource after 15 years. *Nucleic Acids Research*. 2015; 43: D213–D221. doi:10.1093/nar/gku1243.
- [26] Li W, Cowley A, Uludag M, Gur T, McWilliam H, Squizzato S, Park YM, Buso N, Lopez R. The EMBL-EBI bioinformatics web and programmatic tools framework. *Nucleic Acids Research*. 2015; 43(W1): W580–W584. doi:10.1093/nar/gkv279.
- [27] McWilliam H, Li W, Uludag M, Squizzato S, Park YM, Buso N, Cowley AP, Lopez R. Analysis tool web services from the EMBL-EBI. *Nucleic Acids Research*. 2013; 41: W597–W600. doi:10.1093/nar/gkt376.
- [28] Combet C, Blanchet C, Geourjon C, Deléage G. NPS@: network protein sequence analysis. *Trends in Biochemical Sciences*. 2000; 25(3): 147–150. doi:10.1016/S0968-0004(99)01540-6.
- [29] Boratyn GM, Camacho C, Cooper PS, Coulouris G, Fong A, Ma N, Madden TL, Matten WT, McGinnis SD, Merezhuk Y, Raytselis Y, Sayers EW, Tao T, Ye J, Zaretskaya I. BLAST: a more efficient report with usability improvements. *Nucleic Acids Research*. 2013; 41: W29–W33. doi:10.1093/nar/gkt282.
- [30] Sigrist CJA, de Castro E, Cerutti L, Cuche BA, Hulo N, Bridge A, Bougueleret L, Xenarios I. New and continuing developments at PROSITE. *Nucleic Acids Research*. 2012; 41: D344–D347. doi:10.1093/nar/gks1067.
- [31] Sigrist CJA, Cerutti L, Hulo N, Gattiker A, Falquet L, Pagni M, Bairoch A, Bucher P. PROSITE: a documented database using patterns and profiles as motif descriptors. *Briefings in Bioinformatics*. 2002; 3: 265–274. <http://bib.oxfordjournals.org/content/3/3/265.long>.
- [32] Suzek BE, Wang Y, Huang H, McGarvey PB, Wu CH, the UniProt Consortium. UniRef clusters: a comprehensive and scalable alternative for improving sequence similarity searches. *Bioinformatics*. 2015; 31(6): 926–932. doi:10.1093/bioinformatics/btu739.
- [33] Ash C, Farrow JA, Dorsch M, Stackebrandt E, Collins MD. Comparative analysis of *Bacillus anthracis*, *Bacillus cereus*, and related species on the basis of reverse transcriptase sequencing of 16SrRNA. *International Journal of Systematic and Evolutionary Microbiology* 1991; 41: 343–346. doi:10.1099/00207713-41-3-343.

- [34] Lechner S, Mayr R, Francis K.P, Pruss BM, Kaplan T, Wiessner-Gunkel E, Stewart GS, Scherer S. *Bacillus weihenstephanensis* sp. Nov. is a new psychrotolerant species of the *Bacillus cereus* group. *International Journal of Systematic and Evolutionary Microbiology*. 1998; 48: 1373–1382. doi:10.1099/00207713-48-4-1373.
- [35] Nakamura LK. *Bacillus pseudomycooides* sp. Nov. *International Journal of Systematic Bacteriology*. 1998; 48: 1031–1035. doi:10.1099/00207713-48-3-1031.
- [36] Agarwala R, Barrett T, Beck J, Benson DA, Bollin C, Bolton E, Bourexis D, Brister JR, Bryant SH, Canese K, Clark K, DiCuccio M, Dondoshansky I, Federhen S, Feolo M, Funk K, Geer LY, Gorelenkov V, Hoepfner M, Holmes B, Johnson M, Khotomlianski V, Kimchi A, Kimelman M, Kitts P, Klimke W, Krasnov S, Kuznetsov A, Landrum MJ, Landsman D, Lee JM, Lipman DJ, Lu Z, Madden TL, Madej T, Marchler-Bauer A, Karsch- Mizrahi I, Murphy T, Orris R, O'Sullivan C, Panchenko A, Phan L, Preuss D, Pruitt KD, Rubinstein W, Sayers EW, Schneider V, Schuler GD, Sherry ST, Sirotkin K, Siyan K, Slotta D, Soboleva A, Soussov V, Starchenko G, Tatusova TA, Trawick BW, Vakatov D, Wang Y, Ward M, Wilbur WJ, Yaschenko E, Zbicz K. Database resources of the national center for biotechnology information. *Nucleic Acids Research*. 2015; 43: D6–D17. doi:10.1093/nar/gku1130.
- [37] Larkin MA, Blackshields G, Brown NP, Chenna R, McGettigan PA, McWilliam H, Valentin F, Wallace IM, Wilm A, Lopez R., Thompson JD, Gibson TJ, Higgins DG. Clustal W and Clustal X version 2.0. 2007; 23(21): 2947–2948. doi:10.1093/bioinformatics/btm404.
- [38] Henikoff S, Henikoff JG. Amino acid substitution matrices from protein blocks. *Proceedings of the National Academy of Sciences USA*. 1992; 89: 10915–10919. <http://www.pnas.org/content/89/22/10915.full.pdf>.
- [39] Tocheva EI, Dekas AE, McGlynn SE, Morris D, Orphan VJ, Jensen GJ. Polyphosphate Storage during sporulation in the Gram-Negative Bacterium *Acetonebacterium longum*. *Journal of Bacteriology*. 2013; 195(17): 3940–3946. doi:10.1128/JB.00712-13.
- [40] Molle V, Fujita M, Jensen ST, Eichenberger P, Gonzalez-Pastor JE, Liu JS, Losick R. The Spo0A regulon of *Bacillus subtilis*. *Mol. Microbiol.* 2003; 50: 1683–1701. doi:10.1046/j.1365-2958.2003.03818.x.
- [41] Bidnenko V, Shi L, Kobir A, Ventroux M, Pigeonneau N, Henry C, Trubuil A, Noirot-Gros MF, Mijakovic I. *Bacillus subtilis* serine/threonine protein kinase YabT is involved in spore development via phosphorylation of a bacterial recombinase. *Molecular Microbiology*. 2013; 88(5): 921–935. doi: 10.1111/mmi.12233.
- [42] Burbulys D, Trach AK, Hoch AJ. The initiation of sporulation in *Bacillus subtilis* is controlled by a multicomponent phosphorelay. *Cell*. 1991; 64: 545–552. doi: 10.1016/0092-8674(91)90238-T.
- [43] Liu J, Tan K, Stormo DG. Computational identification of the Spo0A-phosphate regulon that is essential for the cellular differentiation and development in Gram-positive

- spore-forming bacteria. *Nucleic Acids Research*. 2003; 31: 6891–6903. doi:10.1093/nar/gkg879.
- [44] Jiang M, Shao W, Perego M, Hoch AJ. Multiple histidine kinases regulate entry into stationary phase and sporulation in *Bacillus subtilis*. *Molecular Microbiology*. 2000; 38: 535–542. doi:10.1046/j.1365-2958.2000.02148.x.
- [45] Kobayashi K, Shoji K, Shimizu T, Nakano K, Sato T, Kobayashi Y. Analysis of a suppressor mutation *ssb* (*kinC*) of *surOB20* (*spo0A*) mutation in *Bacillus subtilis* reveals that *kinC* encodes a histidine protein kinase. *Journal of Bacteriology*. 1995; 177: 176–182. <http://jb.asm.org/content/177/1/176.long>.
- [46] LeDeaux RJ, Grossman AD. Isolation and characterization of *kinC*, a gene that encodes a sensor kinase homologous to the sporulation sensor kinases KinA and KinB in *Bacillus subtilis*. *Journal of Bacteriology*. 1995; 177:166–175. <http://jb.asm.org/content/177/1/166.full.pdf>.
- [47] LeDeaux, RJ, Yu N, Grossman AD. Different roles for KinA, KinB, and KinC in the initiation of sporulation in *Bacillus subtilis*. *Journal of Bacteriology*. 1995; 177: 861–863. <http://www.ncbi.nlm.nih.gov/pmc/articles/PMC176674/pdf/1770861.pdf>.
- [48] Crawford NM, Glass ADM. Molecular and physiological aspects of nitrate uptake in plants. *Trends Plant Science*. 1998; 3: 389–395. doi:10.1016/S1360-1385(98)01311-9.
- [49] Blumwald E, Poole RJ. Nitrate storage and retrieval in *Beta vulgaris*: effects of nitrate and chloride on proton gradients in tonoplast vesicles. *Proceedings of the National Academy of Sciences USA*. 1985; 82: 3683–3687. <http://www.ncbi.nlm.nih.gov/pmc/articles/PMC397851/?page=1>.
- [50] Yokoyama K, Imamura H. Rotation, structure, and classification of prokaryotic V-ATPase. *Journal of Bioenergetics and Biomembranes*. 2005; 37: 405–410. doi:10.1007/s10863-005-9480-1.
- [51] Maeshima M. Vacuolar H_p-pyrophosphatase. *Biochimica et Biophysica Acta*. 2000; 1465: 37–51. doi:10.1016/S0005-2736(00)00130-9.
- [52] Mußmann M, Hu ZF, Richter M, Beer DD, Preisler A, Jørgensen BB, Huntemann M, Glockner OF, Amann R, Koopman JHW, Lasken SR, BenjaminJanto, Hogg J, Stoodley P, Boissy R, Ehrlich DG. Insights into the genome of large sulfur bacteria revealed by analysis of single filaments. *Plos Biology*. 2007; 5(9): 230. doi:10.1371/journal.pbio.0050230.